

Article

Linked Color Imaging of Barrett's Esophageal Adenocarcinoma: Effects on Visibility

Masahiro Saito ^{1,2,*}, Tomoyuki Koike ¹, Yuki Ohara ¹, Yohei Ogata ¹, Takeshi Kanno ¹, Xiaoyi Jin ¹, Waku Hatta ¹, Kaname Uno ¹, Naoki Asano ¹, Akira Imatani ¹ and Atsushi Masamune ¹

¹ Division of Gastroenterology, Tohoku University Graduate School of Medicine, Sendai 980-8575, Japan

² Department of Community Medical Supports, Tohoku Medical Megabank Organization, Tohoku University, Sendai 980-8573, Japan

* Correspondence: sitmshr@gmail.com

Abstract: Since linked color imaging (LCI) has been reported to increase the color differences in Barrett's esophageal adenocarcinoma (BA) compared to white light imaging (WLI), a comparison of the visibility scores of various imaging techniques for BA is warranted to determine best practice standards. This study is to clarify the role of LCI, blue light imaging (BLI), and WLI in the evaluation of BA. A group of 19 endoscopists, comprised of 6 experts and 13 trainees, evaluated the visibility of WLI, BLI, and LCI images in 21 superficial BA cases. Visibility scores were compared between WLI, BLI, and LCI. Visibility scores were also evaluated for lesion morphology, background Barrett's mucosa, and circumferential location. The visibility scores of experts and trainees were analyzed for comparison. The visibility scores of LCI and BLI were 3.83 and 3.31, respectively, compared to three points for WLI. The visibility of LCI was better than that of WLI regardless of lesion morphology, color, background Barrett's mucosa, and circumferential location. The LCI improved visibility in BA more than the WLI for both experts and trainees. LCI improved the visibility of BA independent of lesion morphology, color, background Barrett's mucosa, circumferential location, and the endoscopist's experience.

Keywords: Barrett's esophageal adenocarcinoma; visibility; blue light imaging; linked color imaging



Citation: Saito, M.; Koike, T.; Ohara, Y.; Ogata, Y.; Kanno, T.; Jin, X.; Hatta, W.; Uno, K.; Asano, N.; Imatani, A.; et al. Linked Color Imaging of Barrett's Esophageal Adenocarcinoma: Effects on Visibility. *Gastroenterol. Insights* **2024**, *15*, 145–155. <https://doi.org/10.3390/gastroent15010010>

Academic Editor: Micheal Tadros

Received: 27 November 2023

Revised: 17 January 2024

Accepted: 1 February 2024

Published: 5 February 2024



Copyright: © 2024 by the authors. Licensee MDPI, Basel, Switzerland. This article is an open access article distributed under the terms and conditions of the Creative Commons Attribution (CC BY) license (<https://creativecommons.org/licenses/by/4.0/>).

1. Introduction

Barrett's esophageal adenocarcinoma (BA) has increased significantly in recent decades in Europe and in the United States, accounting for more than half of all esophageal cancers and becoming a more prevalent disease [1]. In Japan, the proportion of esophageal cancers is still small, but it is increasing, and it is expected to become even more prevalent in the future [2,3].

BA has a poor prognosis because of the high rate of lymph node metastasis in advanced cancer. When diagnosed at the stage at which the BA causes symptoms, the prognosis is poor [4]. Since BA has a poor prognosis when detected at an advanced stage, early detection is beneficial, not only because it can be treated with a low-risk, minimally invasive endoscopic resection but also because it has a good prognosis [5,6]. Endoscopic observation of high-risk patients for the early detection of BA is a significant risk reduction strategy that deserves consideration.

Endoscopic surveillance of high-risk patients, while theoretically beneficial, is a challenging endeavor, as the diagnosis of superficial BA on endoscopy can be difficult [3,7]. In recent years, the linked color imaging (LCI) system has been developed as a new endoscopic imaging modality [8,9]. In addition to color enhancement, LCI uses a short wavelength of 410 nm in addition to white light imaging (WLI), which reflects superficial mucosal and vascular structures in LCI [9]. LCI has been reported to be useful in the early detection of gastrointestinal tumors. Prior reports have found that LCI increases color differences and

visibility in gastric cancer, colorectal neoplasia, and duodenal tumors [10–14]. Recently, LCI has also been found to be beneficial in the endoscopic detection of both neoplastic lesions and inflammatory lesions such as reflux esophagitis and eosinophilic esophagitis [15,16].

The advantages of LCI in the diagnosis of gastrointestinal cancer have been demonstrated in the large study “LCI-FIND trial” [17]. LCI is useful in identifying neoplastic lesions even when used in ultraslim endoscopy due to its’ high lesion recognition [18]. However, all esophageal cancers were only squamous cell carcinoma (SCC) or intraepithelial neoplasia. An examination of visibility for BA is warranted.

In BA, as in other gastrointestinal cancers, we have reported that the color difference increases in LCI compared to WLI [19]. The improvements were seen in the color difference with LCI, although this study did not determine if visibility was improved with LCI in patients with BA. Few reports have examined the visibility of BA in LCI [20,21]. Moreover, the relationship between color difference and visibility has not been reported. In this study, we examined the color differences from the viewpoint of visibility, adding objective evidence with the color difference to examine the relationship between color difference and visibility. A statistical analysis of the utility of LCI for experts in comparison to trainees is also of interest.

This study was designed to detect changes in the visibility of BA from WLI, BLI, and LCI, to detect the effect LCI has on visibility, and to evaluate the association between color differences (ΔE^*) and visibility scores.

2. Materials and Methods

2.1. Materials for Visibility Evaluation

We used endoscopic images of 21 consecutive BA cases, all of which were observed endoscopically before endoscopic treatment, from November 2014 to September 2017 [19]. Inclusion criteria were cases who underwent endoscopic treatment for superficial BA and had all WLI, BLI, and LCI images and images from the same position that could be compared. Cases with advanced BA were excluded because advanced BA is more easily recognized. The endoscopic images with WLI, BLI, and LCI recorded in the filing system were retrospectively evaluated. The endoscopic images taken from approximately the same position on the captured image were selected and extracted in a fully extended condition, without magnification.

A total of 21 images were extracted and prepared for each modality to be presented consecutively to endoscopists for interpretation. The images were prepared to show to each endoscopist on a black background on a PowerPoint® (Microsoft Corporation, Redmond, WA, USA) screen without detailed information about the case [20,22].

2.2. Esophagogastroduodenoscopy and Endoscopic Findings

Esophagogastroduodenoscopies (EGD) were performed using a high-definition EG-L600WR or EG-L600ZW endoscope corresponding to the LASEREO® endoscopic system (FUJIFILM Co., Tokyo, Japan).

The following endoscopic findings of the BA were evaluated by two endoscopic experts certified by the Japan Gastroenterological Endoscopy Society (JGES). The esophagogastric junction (EGJ) was defined endoscopically as the lower margin of palisading vessels according to the Japanese Classification of Esophageal Cancer, 11th Edition [23,24]. If the palisading small vessels were unclear, the oral margin of the longitudinal folds of the greater curvature of the stomach was defined as the EGJ. An esophagus containing Barrett’s mucosa has an inherent risk of progression to BA. According to the Japanese Classification of Esophageal Cancer, 11th Edition, Barrett’s mucosa is a columnar epithelium continuous from the stomach. BA was defined as adenocarcinoma arising in Barrett’s mucosa [23,24].

Cases diagnosed as having Barrett’s mucosa extending longitudinally ≥ 3 cm were subgrouped as long-segment BE (LSBE), and those who were diagnosed as having Barrett’s mucosa extending to < 3 cm from the EGJ were subgrouped as short-segment BE (SSBE) [23,24]. The diameter of the BA was measured on the resected specimen. The macro-

scopic form of BA was diagnosed endoscopically and classified as the protruding type, or the flat or depressed type, based on the Paris classification. The color of the lesions was classified into reddish lesions and normal to otherwise discolored lesions. The localization with respect to the circumference was classified into two types: lesions in the 0–3 o'clock direction of the EGJ and in all other directions.

2.3. Evaluator of Visibility Score

Nineteen endoscopists compared the prepared WLI, LCI, and BLI images and gave visibility scores. Moreover, 6 of the 19 were experts, and 13 were trainees. The experts were endoscopists certified by JGES, while the trainees did not have this certification.

2.4. Scoring for Visibility

The endoscopist scored a visibility score on the prepared images for each BA case [20]. Each endoscopist viewed the prepared images in random order on a PowerPoint® with a black background. WLI-LCI or WLI-BLI images were displayed side by side. Based on the previously reported scores on WLI of 3 points, the visibility was scored as 1 through 5 as follows: 1 (substantially decreased), 2 (marginally decreased), 3 (no change), 4 (marginally improved), and 5 (substantially improved) as in the reports that evaluated the visibility by a method of evaluating improvement to deterioration on a 5-point scale for LCI and BLI [10,15,22]. The average score was calculated for each lesion after all endoscopists completed the scoring.

2.5. Comparing Visibility Scores and Color Difference (ΔE^*)

We statistically analyzed the visibility score of BLI and LCI for WLI for each lesion. The visibility score was analyzed according to the morphology of lesions (protruding type/flat or depressed type), the color of the lesions (reddish lesions/normal to discolored lesions), the length of the background Barrett's mucosa (SSBE/LSBE), and the localization with respect to the circumference (0–3 o'clock directions/all other directions). The visibility score was also analyzed according to the type of examiner (experts/trainees).

Furthermore, the relationship between the ΔE^* value and the visibility score was investigated to determine relevance. The region of interest (ROI) was selected inside and outside of the BA lesion, and the average of the absolute color values in the ROI was calculated using image analysis software (Adobe Photoshop CC® 2017; Adobe Systems, San Jose, CA, USA). L , a , and b color values were transformed into $L^*a^*b^*$ color values as follows: $L^* = L/256 \times 100$, $a^* = a - 128$, and $b^* = b - 128$. The ΔE^* between BA and surrounding Barrett's mucosa was calculated in accordance with the previously reported method based on the $L^*a^*b^*$ color spaces ($\Delta E^* = ((\Delta L^*)^2 + (\Delta a^*)^2 + (\Delta b^*)^2)^{1/2}$) [11,12,19]. The ΔE^* values were divided into two groups based on the mean value of the visibility score of LCI as assessed by the endoscopists. Lesions with 3 to 4 points were categorized as "slightly improved group", whereas lesions with >4 points were categorized as "largely improved group". The ΔE^* value in WLI and LCI was compared in both groups. To examine the relationship between visibility and color difference in BA, we conducted a correlation analysis. The differences in the ΔE^* value between LCI and WLI were calculated and expressed as " $\Delta E^*_{(LCI)} - \Delta E^*_{(WLI)}$ ". Thereafter, we correlated this color difference with the visibility score.

The study was approved by the Ethics Committee of Tohoku University Graduate School of Medicine (Protocol Identification Number 2020-1-798).

2.6. Statistical Analysis

This study was the first to examine the visibility of LCI for BA; hence, it was difficult to calculate the sample size in advance. Post hoc, however, we sufficiently detected significant differences in visibility and the correlation between visibility and color differences in 21 cases. Baseline data are presented as the mean (\pm standard deviation (SD)). Data management and statistical analysis were performed using EZR (Saitama Medical Center,

Jichi Medical University, Saitama, Japan), a graphical user interface for R (The R Foundation for Statistical Computing, Vienna, Austria) [25]. Parameters between any combinations of two groups were analyzed with the Wilcoxon signed-rank test. Categorical variables in the patients' backgrounds were compared using Fisher's exact test. The correlation coefficient between the difference in the visibility score and the color difference was calculated, and the significant difference ratio was calculated using Pearson's product-moment correlation coefficient because both values were in a normal distribution. A *p*-value of <0.05 was considered to be statistically significant. The inter-rater reliability (internal consistency) was measured using the Cronbach's alpha statistic.

3. Results

Nine lesions (42.9%) were classified as protruding lesions, and 12 lesions (57.1%) were classified as flat or depressed. The majority (18; 85.7%) were reddish in color, and the remaining 3 lesions were either a similar color to the surroundings or otherwise discolored. Moreover, 17 of 21 lesions were SSBE. The majority (17; 80.9%) of the lesions were located in the 0–3 o'clock direction, and four lesions (19.1%) were found in other directions. The median interquartile range (IQR) diameter of the targeted lesions was 14 mm (11 mm) (Table 1).

Table 1. Characteristics of 21 targeted lesions.

Parameter		Value	
Total lesions (<i>n</i> = 21)			
Color	Reddish	18	(85.7%)
	Similar color to the surroundings or discolored	3	(14.3%)
Form	Protruding	9	
	Type 0—I	3	(14.3%)
	Type 0—IIa	5	(23.8%)
	Type 0—IIa + IIc	1	(4.8%)
	Flat or depressed	12	
	Type 0—IIb	2	(9.5%)
Barrett's mucosa	Type 0—IIc	10	(47.6%)
	SSBE	17	(80.9%)
	LSBE	4	(19.1%)
Circumferential location	0–3 o'clock direction	17	(80.9%)
	Other direction	4	(19.1%)
The diameter of the lesions	mm, median (IQR)	14 (11)	

SSBE—short-segment Barrett's esophagus; LSBE—long-segment Barrett's esophagus; IQR—interquartile range.

The mean visibility score on LCI for all 21 BA lesions is 3.83 (± 0.44), with visibility on WLI of 3 points. The mean BLI visibility score is 3.31 (± 0.47). The visibility scores of LCI and BLI are statistically significantly higher compared with WLI ($p < 0.0001$ and $p < 0.01$, respectively). The visibility of LCI is also statistically significantly higher than that of BLI ($p < 0.001$) (Figure 1).

In the examination by macroscopic type of lesion, in the nine protruding lesions, the visibility score of BLI is 3.08 (± 0.50), which is not statistically different compared with WLI ($p = 0.86$). The visibility score of LCI is 3.73 (± 0.52), which is significantly higher than that of both WLI and BLI ($p < 0.01$ and $p < 0.05$, respectively) (Figure 2A).

In the 12 flat to depressed lesions, the visibility score of BLI is 3.48 (± 0.37), which is significantly higher than that of WLI ($p < 0.01$). The visibility score of LCI is 3.91 (± 0.37), which is significantly higher than that of WLI and BLI ($p < 0.01$ and $p < 0.01$, respectively) (Figure 2B).

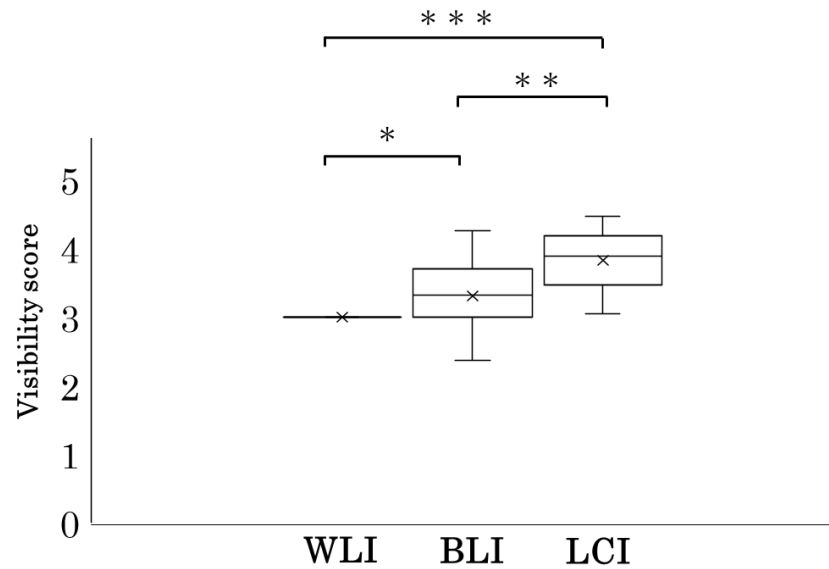


Figure 1. The visibility score on LCI and BLI for all 21 BA lesions compared with visibility on WLI of three points is presented. Statistically, significant differences are observed between WLI and LCI, between BLI and LCI, and between WLI and BLI. * $p < 0.01$, ** $p < 0.001$, and *** $p < 0.0001$. WLI—white light imaging; BLI—blue light imaging; LCI—linked color imaging.

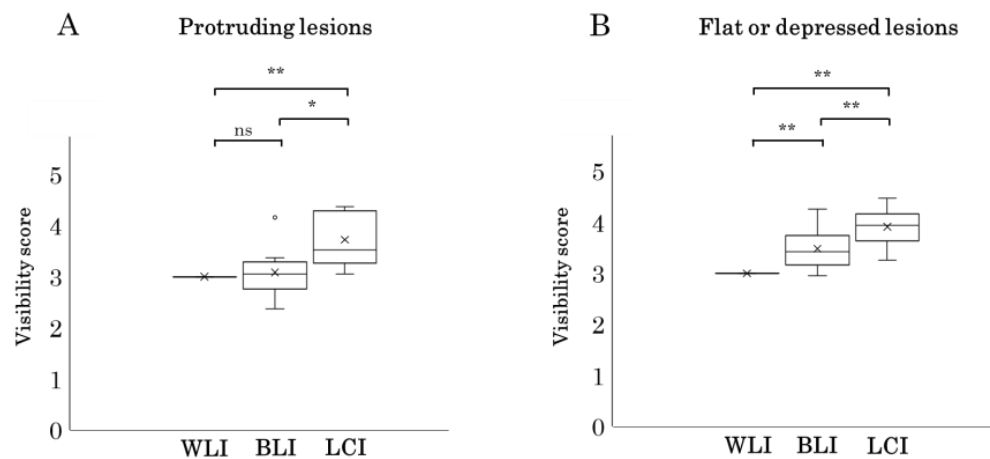


Figure 2. Comparisons of visibility scores by lesion morphology are presented. (A) The visibility scores in the protruding lesion. Statistically, significant differences are observed between WLI and LCI and between BLI and LCI. A significant difference between WLI and BLI is not observed. (B) The visibility scores in the flat or depressed lesions. Statistically, significant differences are observed between WLI and LCI, between BLI and LCI, and between WLI and BLI. * $p < 0.05$, ** $p < 0.01$, ns, not significant. WLI—white light imaging; BLI—blue light imaging; LCI—linked color imaging.

All 18 reddish lesion cases are assigned the highest visibility score in LCI compared with WLI and BLI. In addition, among the three discolored lesions, two cases have the highest LCI visibility score. In cases with background Barrett’s mucosa, LCI has the highest visibility score in all 17 SSBE cases and in 3 out of 4 cases (75%) of LSBE. Regarding the location of lesions, LCI has the highest visibility score in all 17 cases existing in the 0–3 o’clock direction and in 3 out of 4 cases (75%) existing in other directions (Table 2).

Table 2. The observation method with the largest visibility score.

Color of the BA Lesion	Reddish (<i>n</i> = 18)	Discolored (<i>n</i> = 3)
WLI	-	-
BLI	-	2 *
LCI	18	2 *
SSBE or LSBE	SSBE (<i>n</i> = 17)	LSBE (<i>n</i> = 4)
WLI	-	-
BLI	1 *	1
LCI	17 *	3
Circumference of the BA Lesion	0–3 O’Clock (<i>n</i> = 17)	Other (<i>n</i> = 4)
WLI	-	-
BLI	1 *	1
LCI	17 *	3

* There is one case with the same score, counted for both observation methods. BA—Barrett’s adenocarcinoma; WLI—white light images; BLI—blue light imaging; LCI—linked color imaging; SSBE—short-segment Barrett’s esophagus; LSBE—long-segment Barrett’s esophagus

The examination results of visibility scores for experts or trainees are presented in Figure 3. The visibility score in experts is 3.81 (± 0.46) and 3.29 (± 0.51) in LCI and BLI, and, in trainees, the visibility scores for LCI and BLI are 3.84 (± 0.47) and 3.36 (± 0.41) ($p < 0.001$, $p < 0.05$, respectively). Both experts and trainees have significantly higher visibility scores for LCI than for BLI and WLI ($p < 0.0001$, $p < 0.01$, respectively) (Figure 3).

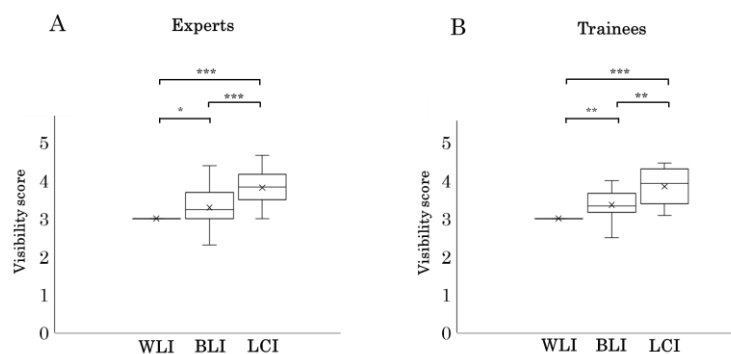


Figure 3. A comparison of the visibility of experts and trainees is presented. (A) The visibility scores by experts. The visibility score on LCI and BLI for all 21 BA lesions is compared with the visibility on WLI of 3 points. Statistically significant differences are observed between WLI and LCI, between BLI and LCI, and between WLI and BLI. (B) The visibility scores of trainees. The visibility score on LCI and BLI for all 21 BA lesions is compared with the visibility on WLI of 3 points. Statistically significant differences are observed between WLI and LCI, between BLI and LCI, and between WLI and BLI. * $p < 0.05$, ** $p < 0.01$, and *** $p < 0.001$. WLI—white light imaging; BLI—blue light imaging; LCI—linked color imaging.

The internal consistency (inter-rater reliability (IRR)) of experts and trainees for visibility scores for LCI were 0.666 and 0.851, respectively. The IRR was good for experts, while it was excellent for trainees.

Based on the LCI visibility score, 11 cases were classified as slightly improved, while the remaining 10 cases were classified as largely improved. For the slightly improved group, the mean ΔE^* value for WLI and LCI was 10.4 points and 15.9 points, respectively. The largely improved group had a mean ΔE^* value of 9.9 points for WLI and 21.5 points for LCI. The color difference in LCI was significantly greater than in WLI in both groups ($p < 0.05$ and $p < 0.01$, respectively; Figure 4).

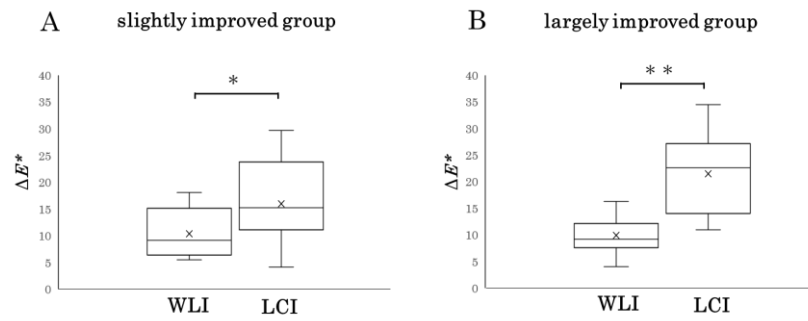


Figure 4. A comparison of the color difference (ΔE^*) in the slightly improved group and in the largely improved group is presented. **(A)** The color difference in the slightly improved group. The ΔE^* value of LCI was significantly greater than that of WLI. **(B)** The color difference in the largely improved group. The ΔE^* value of LCI was significantly greater than that of WLI. * $p < 0.05$, ** $p < 0.01$. WLI—white light imaging; LCI—linked color imaging.

The correlation between the difference in ΔE^* value ($\Delta E^*_{(LCI)} - \Delta E^*_{(WLI)}$) in the 21 lesions and the difference in the visibility score (LCI – WLI) is presented in Figure 5. There was a positive correlation [correlation coefficient (r) of 0.44] between the visibility score difference and the difference in ΔE^* value ($\Delta E^*_{(LCI)} - \Delta E^*_{(WLI)}$) ($p < 0.05$).

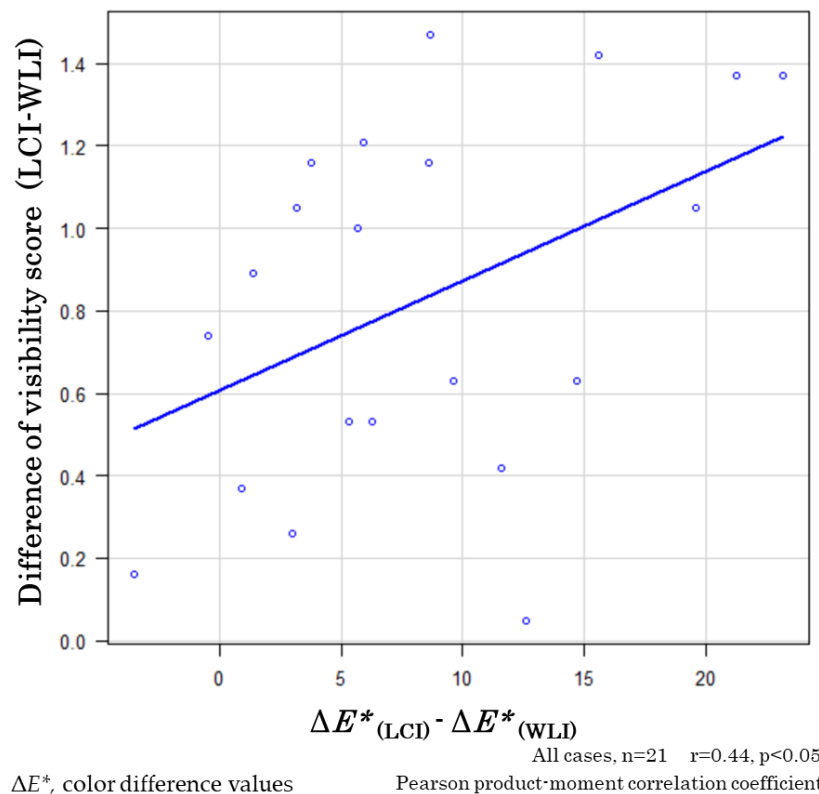


Figure 5. The correlation coefficient between the difference in ΔE^* value ($\Delta E^*_{(LCI)} - \Delta E^*_{(WLI)}$) and the differences in the visibility score (LCI – WLI) is presented. A statistically significant positive correlation coefficient (r) of 0.44 was observed ($p < 0.05$). WLI—white light imaging; LCI—linked color imaging.

The representative images of WLI and LCI in this study are presented along with color differences and visibility scores in Figure 6.

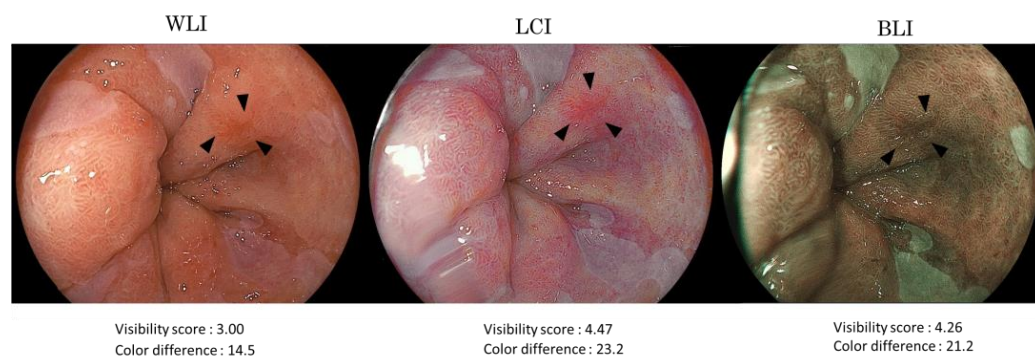


Figure 6. The representative images of WLI and LCI in this study are presented. The visibility score is the mean value of the 19 endoscopists. The values of the color difference (ΔE^*) between the inside and outside of the lesion are also presented. Three arrowheads in each image indicate the BA lesion (there are no arrows in the images shown in the endoscope when comparing the actual visibility scores). WLI—white light imaging; BLI—blue light imaging; LCI—linked color imaging.

4. Discussion

In this study, we found that LCI increases the visibility of BA. BLI also contributes to improving visibility; however, LCI provides better visibility than BLI or WLI. Furthermore, LCI visibility of BA is excellent regardless of the form of the lesion, color, degree of background Barrett's mucosa (SSBE/LSBE), or circumferential location. LCI increased the visibility of BA compared with WLI for both experts and trainees. More importantly, the improvement in visibility was correlated and related to the difference in ΔE^* value as an objective numerical value as a result of evaluating the color difference together.

LCI of the LASEREO[®] system is a laser light system that has been developed to provide image enhancement during endoscopy. LCI uses a wavelength of 410 ± 10 nm, which reflects in the blood vessels and in the microscopic structure of the mucosal surface layer, as well as white light with a longer wavelength of 450 ± 10 nm, which reflects in the deeper structures of the mucosa. Therefore, LCI enhances imaging of the vascular and surface structures. The LCI light is also color-processed on the obtained images. These factors together increase the color difference [8,9]. By expanding the color difference, LCI is expected to make the lesion more easily visible and more distinct from the surrounding mucosa. It has been previously reported in gastric cancer and in neoplasms of the colon and duodenum that LCI is useful in surveillance by increasing the color difference [10–14]. Previous reports have also documented that LCI also improves the visibility of Barrett's mucosa in the esophagus [20,22].

Previous studies found that LCI increases the color difference between the BA lesion and the surrounding Barrett's mucosa in the $L^*a^*b^*$ color space [19,20]. The color difference was greatest in the LCI observation in >80% of the cases. The $L^*a^*b^*$ color space is currently the most widely used color system for representing the colors of objects in all fields [11,12]. Although the color difference is nearly identical to human perception, an examination of visibility scoring for BA is warranted. We not only examined BA using the visibility score widely used to assess the visibility of LCI in lesions at other sites [10–14] but also evaluated the correlation between color difference values and visibility difference values.

This study found that LCI has a higher visibility than WLI, and thus, LCI is considered the best observation method for BA regardless of lesion morphology, color, or location. As for the circumferential location, we divided BA into two groups (0–3 o'clock direction and the other direction groups). This is because BA is reported to develop more frequently in the 0–3 o'clock direction in Japan. We also examined the visibility in relation to the endoscopist's experience. Our results show that experts and trainees improve their visibility with LCI. Therefore, LCI is useful to specialists and non-specialists. It is expected that early detection of BA will be easier for non-specialists because LCI improves visibility regardless of endoscopist experience. It is also important for specialists to spare no effort in switching to LCI for more reliable diagnosis. In terms of the color difference (ΔE^*) value, the color

difference in LCI was significantly greater than in WLI in the slightly improved and largely improved groups, which supports the result of improved visibility.

Multiple prior reports have documented that LCI improves the color difference and visibility of cancer or neoplasia in the upper gastrointestinal tract, including the stomach and the duodenum [10–12,14]. The advantages of LCI in the diagnosis of gastrointestinal cancer were demonstrated in a large study, the “LCI-FIND trial”, and it was reported that LCI is more effective than WLI in esophageal squamous cell carcinoma (ESCC) or intraepithelial neoplasia [17]. In other reports on ESCC, the detection rates of ESCC did not significantly differ between BLI and LCI [26].

For esophageal adenocarcinoma (EAC), in a previous report, Tokunaga et al. evaluated 12 cases of EAC by three specialists and three trainees and reported that LCI had good visibility [20]. As shown in the previous section, regarding ESCC, there are reports that LCI was better than WLI, but there was no difference from BLI [17,26]. For EAC, Tokunaga et al.’s study found no difference between LCI and BLI [20]. This is probably because Tokunaga et al.’s study involved a small number of cases. In our study, we evaluated 21 cases of superficial BAs and found that LCI has good visibility for both WLI and BLI for esophageal BA.

Additionally, we found that LCI proves beneficial irrespective of the lesion’s form, whether it is protruding, flat, or depressed. Furthermore, in this study, the IRR for specialists (6 endoscopists) was 0.666, considered good, and the IRR for non-specialists (13 endoscopists) was 0.851, considered excellent. Another strength of this paper is that we were able to conduct evaluations with less variation between examiners, although the number of both specialists and trainees was larger than in the previous report [20].

Another important strength of this study is how endoscopists’ visibility relates to objectively measured and calculated color difference values. There are no known previous studies that have examined the relationship between the color difference of individual lesions and the visibility score. By evaluating the correlation between the difference in visibility score (LCI – WLI) and ΔE^* value in this study, we found a significant positive correlation. Color differences are universally used in the evaluation of industrial products. Although the numerical value of ΔE^* is close to the visibility of the human eye, there is no report showing its relevance in endoscopic observation. Our findings indicate that LCI improves the visibility of endoscopists by improving the color difference. This could offer a benefit in the detection of cancerous and precancerous lesions in other sites and thus warrant further investigation.

This study had some limitations. First, our sample size was small, and the reason is that there are few cases of superficial BA in Japan and only a limited number of cases for which comparable WLI, BLI, or LCI images from the same position exist. A larger study is required. There is another limitation that the endoscopist already knows from the beginning about the existence of lesions, which may lead to a bias in the evaluation of visibility, although this study was conducted using a scoring method similar to the study of visibility in other gastrointestinal cancers.

Adenocarcinoma is increasing in esophageal cancer; hence, it deserves equal attention as SCC [1–3]. For the early detection of BA, LCI may be useful through improved visibility. LCI is a very convenient method that can be switched by simply pressing a button on the endoscope, so it may facilitate the detection of lesions by combining it with other observation methods.

5. Conclusions

LCI improves the visibility of BA independent of the lesion morphology, the color of the lesion, the degree of background Barrett mucosa, and the circumferential location of the lesion, both for expert endoscopists and for trainees.

Author Contributions: Conceptualization, M.S. and T.K. (Tomoyuki Koike); investigation, M.S. and Y.O. (Yuki Ohara); resources, M.S., T.K. (Tomoyuki Koike), T.K. (Takeshi Kanno), Y.O. (Yohei Ogata), X.J., W.H., K.U., N.A. and A.I.; data curation M.S. and Y.O. (Yuki Ohara); writing—original draft preparation, M.S.; writing—review and editing, M.S., N.A. and T.K. (Tomoyuki Koike); supervision, A.M.; project administration, A.M.; funding acquisition, T.K. (Tomoyuki Koike). All authors have read and agreed to the published version of the manuscript.

Funding: This research is funded by FUJIFILM Corporation (J190001877).

Institutional Review Board Statement: The study was conducted according to the guidelines of the Declaration of Helsinki and approved by the Ethics Committee of the Tohoku University School of Medicine (Protocol Identification Number 2020-1-798).

Informed Consent Statement: Informed consent was obtained in the form of opt-out on the website of Tohoku University School of Medicine.

Data Availability Statement: The data that support the findings of this study are available from the corresponding author, M.S., upon reasonable request.

Conflicts of Interest: Dr. Koike received collaboration research funding from Fujifilm Corporation. All other authors disclosed no financial relationships relevant to this publication. The funders had no role in the design of the study; in the collection, analyses, or interpretation of data; in the writing of the manuscript, or in the decision to publish the results.

References

1. Pohl, H.; Sirovich, B.; Welch, H.G. Esophageal adenocarcinoma incidence: Are we reaching the peak? *Cancer Epidemiol. Biomark. Prev.* **2010**, *19*, 1468–1470. [[CrossRef](#)]
2. Matsuno, K.; Ishihara, R.; Ohmori, M.; Iwagami, H.; Shichijyo, S.; Maekawa, A.; Kanesaka, T.; Yamamoto, S.; Takeuchi, Y.; Higashino, K.; et al. Time trends in the incidence of esophageal adenocarcinoma, gastric adenocarcinoma, and superficial esophagogastric junction adenocarcinoma. *J. Gastroenterol.* **2019**, *54*, 784–791. [[CrossRef](#)]
3. Koike, T.; Saito, M.; Ohara, Y.; Hatta, W.; Masamune, A. Current status of surveillance for Barrett's esophagus in Japan and the West. *DEN Open* **2022**, *13*, e94. [[CrossRef](#)]
4. Hur, C.; Miller, M.; Kong, C.Y.; Dowling, E.C.; Nattinger, K.J.; Dunn, M.; Feuer, E.J. Trends in esophageal adenocarcinoma incidence and mortality. *Cancer* **2013**, *119*, 1149–1158. [[CrossRef](#)] [[PubMed](#)]
5. Ishihara, R.; Goda, K.; Oyama, T. Endoscopic diagnosis and treatment of esophageal adenocarcinoma: Introduction of Japan Esophageal Society classification of Barrett's esophagus. *J. Gastroenterol.* **2019**, *54*, 1–9. [[CrossRef](#)] [[PubMed](#)]
6. Probst, A.; Aust, D.; Märkl, B.; Anthuber, M.; Messmann, H. Early esophageal cancer in Europe: Endoscopic treatment by endoscopic submucosal dissection. *Endoscopy* **2015**, *47*, 113–121. [[CrossRef](#)] [[PubMed](#)]
7. Thosani, N.; Abu Dayyeh, B.K.; Sharma, P.; Aslanian, H.R.; Enestvedt, B.K.; Komanduri, S.; Manfredi, M.; Navaneethan, U.; Maple, J.T.; Pannala, R.; et al. ASGE Technology Committee systematic review and meta-analysis assessing the ASGE Preservation and incorporation of valuable endoscopic innovations thresholds for adopting realtime imaging-assisted endoscopic targeted biopsy during endoscopic surveillance of Barrett's esophagus. *Gastrointest. Endosc.* **2016**, *83*, 684–698.
8. Shinozaki, S.; Osawa, H.; Hayashi, Y.; Lefor, A.K.; Yamamoto, H. Linked Color Imaging for the Detection of Early Gastrointestinal Neoplasms. *Ther. Adv. Gastroenterol.* **2019**, *12*, 1756284819885246. [[CrossRef](#)] [[PubMed](#)]
9. Osawa, H.; Miura, Y.; Takezawa, T.; Ino, Y.; Khurelbaatar, T.; Sagara, Y.; Lefor, A.K.; Yamamoto, H. Linked Color Imaging and Blue Laser Imaging for Upper Gastrointestinal Screening. *Clin. Endosc.* **2018**, *51*, 513–526. [[CrossRef](#)] [[PubMed](#)]
10. Yoshifuku, Y.; Sanomura, Y.; Oka, S.; Kurihara, M.; Mizumoto, T.; Miwata, T.; Urabe, Y.; Hiyama, T.; Tanaka, S.; Chayama, K. Evaluation of the visibility of early gastric cancer using linked color imaging and blue laser imaging. *BMC Gastroenterol.* **2017**, *17*, 150. [[CrossRef](#)] [[PubMed](#)]
11. Kanzaki, H.; Takenaka, R.; Kawahara, Y.; Kawai, D.; Obayashi, Y.; Baba, Y.; Sakae, H.; Gotoda, T.; Kono, Y.; Miura, K.; et al. Linked color imaging (LCI), a novel image-enhanced endoscopy technology, emphasizes the color of early gastric cancer. *Endosc. Int. Open* **2017**, *5*, E1005–E1013. [[CrossRef](#)] [[PubMed](#)]
12. Fukuda, H.; Miura, Y.; Osawa, H.; Takezawa, T.; Ino, Y.; Okada, M.; Khurelbaatar, T.; Lefor, A.K.; Yamamoto, H. Linked color imaging can enhance recognition of early gastric cancer by high color contrast to surrounding gastric intestinal metaplasia. *J. Gastroenterol.* **2019**, *54*, 396–406. [[CrossRef](#)] [[PubMed](#)]
13. Paggi, S.; Mogavero, G.; Amato, A.; Rondonotti, E.; Andrealli, A.; Imperiali, G.; Lenoci, N.; Mandelli, G.; Terreni, N.; Conforti, F.S.; et al. Linked color imaging reduces the miss rate of neoplastic lesions in the right colon: A randomized tandem colonoscopy study. *Endoscopy* **2018**, *50*, 396–402. [[PubMed](#)]
14. Okimoto, K.; Maruoka, D.; Matsumura, T.; Tokunaga, M.; Kaneko, T.; Oura, H.; Akizue, N.; Ohta, Y.; Saito, K.; Arai, M.; et al. Linked color imaging can improve the visibility of superficial non-ampullary duodenal epithelial tumors. *Sci. Rep.* **2020**, *10*, 20667. [[CrossRef](#)] [[PubMed](#)]

15. Takeda, T.; Asaoka, D.; Abe, D.; Suzuki, M.; Nakagawa, Y.; Sasaki, H.; Inami, Y.; Ikemura, M.; Utsunomiya, H.; Oki, S.; et al. Linked color imaging improves visibility of reflux esophagitis. *BMC Gastroenterol.* **2020**, *20*, 356. [[CrossRef](#)] [[PubMed](#)]
16. Abe, Y.; Sasaki, Y.; Yagi, M.; Mizumoto, N.; Onozato, Y.; Kon, T.; Shoji, M.; Sakuta, K.; Sakai, T.; Umehara, M.; et al. Linked color imaging improves the diagnostic accuracy of eosinophilic esophagitis. *DEN Open* **2022**, *3*, e146. [[CrossRef](#)] [[PubMed](#)]
17. Ono, S.; Kawada, K.; Dohi, O.; Kitamura, S.; Koike, T.; Hori, S.; Kanzaki, H.; Murao, T.; Yagi, N.; Sasaki, F.; et al. Linked Color Imaging Focused on Neoplasm Detection in the Upper Gastrointestinal Tract: A Randomized Trial. *Ann. Intern. Med.* **2021**, *174*, 18–24. [[CrossRef](#)] [[PubMed](#)]
18. Haruma, K.; Kato, M.; Kawada, K.; Murao, T.; Ono, S.; Suehiro, M.; Hori, S.; Sasaki, F.; Koike, T.; Kitamura, S.; et al. Diagnostic ability of linked color imaging in ultraslim endoscopy to identify neoplastic lesions in upper gastrointestinal tract. *Endosc. Int. Open* **2022**, *10*, E88–E95. [[CrossRef](#)]
19. Saito, M.; Koike, T.; Ohara, Y.; Nakagawa, K.; Kanno, T.; Jin, X.; Hatta, W.; Uno, K.; Asano, N.; Imatani, A.; et al. Linked-color imaging may help improve the visibility of superficial Barrett’s esophageal adenocarcinoma by increasing the color difference. *Intern. Med.* **2021**, *60*, 3351–3358. [[CrossRef](#)]
20. Tokunaga, M.; Matsumura, T.; Ishikawa, K.; Kaneko, T.; Oura, H.; Ishikawa, T.; Nagashima, A.; Shiratori, W.; Okimoto, K.; Akizue, N.; et al. The efficacy of linked color imaging in the endoscopic diagnosis of Barrett’s esophagus and esophageal adenocarcinoma. *Gastroenterol. Res. Pract.* **2020**, *2020*, 9604345. [[CrossRef](#)]
21. de Groof, A.J.; Fockens, K.N.; Struyvenberg, M.R.; Pouw, R.E.; Weusten, B.L.; Schoon, E.J.; Mostafavi, N.; Bisschops, R.; Curvers, W.L.; Bergman, J.J. Blue-light imaging and linked-color imaging improve visualization of Barrett’s neoplasia by nonexpert endoscopists. *Gastrointest. Endosc.* **2020**, *91*, 1050–1057. [[CrossRef](#)]
22. Takeda, T.; Nagahara, A.; Ishizuka, K.; Okubo, S.; Haga, K.; Suzuki, M.; Nakajima, A.; Komori, H.; Akazawa, Y.; Izumi, K.; et al. Improved visibility of Barrett’s esophagus with linked color imaging: Inter- and intra-rater reliability and quantitative analysis. *Digestion* **2018**, *97*, 183–194. [[CrossRef](#)]
23. Japan Esophageal Society. Japanese Classification of Esophageal Cancer, 11th Edition: Part I. *Esophagus* **2017**, *14*, 1–36. [[CrossRef](#)] [[PubMed](#)]
24. Japan Esophageal Society. Japanese Classification of Esophageal Cancer, 11th Edition: Part II and III. *Esophagus* **2017**, *14*, 37–65. [[CrossRef](#)] [[PubMed](#)]
25. Kanda, Y. Investigation of the freely-available easy-to-use software “EZ R” (Easy R) for medical statistics. *Bone Marrow Transplant.* **2013**, *48*, 452–458. [[CrossRef](#)] [[PubMed](#)]
26. Ogata, Y.; Hatta, W.; Koike, T.; Takahashi, S.; Matsuhashi, T.; Oikawa, T.; Iwai, W.; Asonuma, S.; Okata, H.; Ohyauchi, M.; et al. Blue light imaging and linked color imaging as a screening mode for esophageal squamous cell carcinoma in high-risk patients: Multicenter randomized trial. *Dig. Endosc.* **2023**, *35*, 835–844. [[CrossRef](#)]

Disclaimer/Publisher’s Note: The statements, opinions and data contained in all publications are solely those of the individual author(s) and contributor(s) and not of MDPI and/or the editor(s). MDPI and/or the editor(s) disclaim responsibility for any injury to people or property resulting from any ideas, methods, instructions or products referred to in the content.